

Robust Controller Synthesis in Automatic Guided Vehicles Applications

P. Martinet, C. Thibaud, B. Thuilot and J. Gallice

Laboratoire des Sciences et Matériaux pour l'Electronique, et d'Automatique.
Université Blaise Pascal de Clermont-Ferrand,
U.M.R. 6602 du C.N.R.S., F-63177 Aubière Cedex, France
E-Mail: Philippe.Martinet@lasmea.univ-bpclermont.fr

Abstract

We are interested in AGV applications since a long time, particularly in the field of car vehicles and agricultural machines. This paper deals with the design of robust lateral controllers expressed directly in the sensor space. We use the camera sensor to extract an image of the position and orientation of the vehicle in regard with the white band, and consider the modelling of the projected line in image space as the sensor signal. The kinematic modelling of the vehicle takes into account a normalization with respect to the vehicle velocity. We analyse the behaviour of lateral controllers designed with a pole assignment technique in presence of pipeline delays in the closed loop and perturbations. We particularly consider the perturbations on the inclination angle of the camera and on the camera height. Due to the problem of oscillations and instability of this approach, we investigate a \mathcal{H}_∞ robust control technique. To validate these approaches we have built an 1/10 scale road and we simulate the behaviour of the vehicle with a cartesian robot. We give some experimental results obtained with our experimental site.

1 Introduction

In the realm of intelligent highways, many AGV applications have retained attention. For instance, we can cite road sign recognition, crossroad and branching of road detection, platooning, automatic car control, obstacle avoidance, and so on . The problem of vehicle control using a camera has been given considerable attention by many authors [15, 3, 16, 8]. We are interested in road following applications [2] and in designing lateral controller [7] since a long time. The first lateral control application was done in 1992 in

collaboration with the french firm PSA. We used a pole assignment approach based on the localization of the vehicle in regard with the white band on the ground. The real experimentation was done successfully, but some problems appear in presence of perturbations on camera inclination angle, camera height and camera roll angle. Due to the difficulty to estimate the absolute configuration of the vehicle, we have preferred to turn towards control design directly in the sensor space [9, 11, 12]. A same technique, was also studied in [13] by means of the *task function approach* [14].

In this paper, we present the modellings of the vehicle and of the scene. We show how to normalize these modellings with respect to the vehicle velocity and establish the state model of the system. We first design a controller in image space using a pole assignment approach, and second using a robust control approach. In both cases, we analyse the effect of perturbations on the closed loop system.

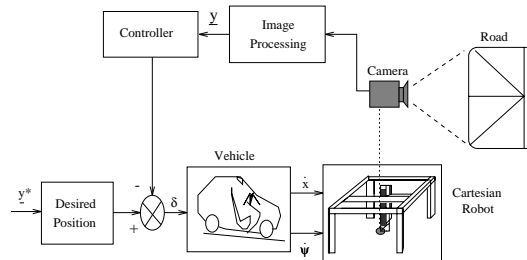


Figure 1: Overview of the experimental site

These approaches were experimented with a 1/10 scale demonstrator (Figure 1). It is composed of a cartesian robot with 6 d.o.f (built by the firm AFMA Robot), a camera mounted on its end effector and the WINDIS parallel vision system. The road built to a 1/10 scale, comprises three white lines.

2 State space modelling

2.1 Modelling the vehicle and the scene

The vehicle is hereafter schematically described using the so-called ‘‘bicycle model’’, see Figure 2. Its position is represented by the couple (x, s) , cartesian coordinates of the center P of the rear wheel, in a referential frame $[O, X, S]$ whose second axle coincides with the straight line (i.e. the white band) to be followed by the vehicle. Its orientation is identified by ψ , the angle between the vehicle axle and $[OS]$, counterclockwise positive.

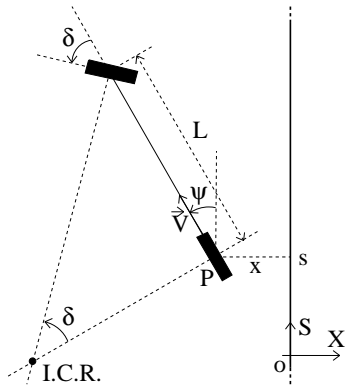


Figure 2: Bicycle model.

The vehicle kinematic equations are derived according to the pure rolling and non-slipping assumptions. These impose that the linear velocity vector at point P , denoted \vec{V} , is directed along the vehicle axle. The time-derivative of x and s are therefore given by :

$$\dot{x} = -V \sin \psi \quad (1)$$

$$\dot{s} = V \cos \psi \quad (2)$$

Let δ be the steering angle, counterclockwise positive, and L be the distance between the front wheel and the rear one. The pure rolling and non-slipping assumptions ensure that the vehicle motion is a translation when $\delta = 0$, and otherwise a rotation about the Instantaneous Center of Rotation (I.C.R.), defined as the intersection of the wheels' axles. In the latter case, when writing the relation between the linear velocity at P and those at the I.C.R., which is zero, it can easily be shown that we have :

$$\psi = \frac{V}{L} \tan \delta \quad (3)$$

Relation 3 is still valid in the former case, since a transition is characterized by $\dot{\psi} = 0$.

Our objective is not to track a point on the reference line, but just to follow this line. We are therefore interested in regulating only x and ψ . Provided that V is never 0, the relation 2 can then be used to normalize the dynamics of x and ψ with respect to the vehicle velocity : let $'$ denote the derivative with respect to the abscissa s . Reporting relation 2 in 1 and 3 and using approximation to small angles leads then to the following vehicle equations :

$$\begin{cases} x' &= -\psi \\ \psi' &= \frac{\delta}{L} \end{cases} \quad (4)$$

Real-time localization of the vehicle is achieved by means of an embedded camera. The height of the camera with respect to the ground, and its inclination angle with respect to the vertical, are hereafter denoted respectively h and α .

The 3D white band of the scene is projected as a 2D line in the camera image frame. Its equation has been shown to be, see [11] :

$$p_x = a p_y + b \quad (5)$$

Approximation to small angles in trigonometric functions in α or ψ has been used. (p_x, p_y) denotes the pixel coordinates of the 2D line in the image frame, and a and b are given by :

$$\begin{cases} a &= \frac{1}{\xi_1} x \\ b &= -\frac{\xi_2}{\xi_1 \xi_3} x + \frac{1}{\xi_3} \psi \end{cases} \quad (6)$$

The constant ξ_1 , ξ_2 and ξ_3 are respectively :

$$\xi_1 = \frac{f_y}{f_x} h \quad \xi_2 = -\frac{f_y}{f_x} \alpha \quad \xi_3 = \frac{1}{f_x}$$

where f_x, f_y are the camera intrinsic parameters ($f_x = 1300pu$, $f_y = 1911pu$, $L = 0.3m$, $h = 0.12m$ and $\alpha = -7^\circ$).

Since we are interested in achieving line following by means of regulation control laws designed in the image frame, a natural state vector for our application is $\underline{Z} = (a, b)^T$. The associated state space model can be obtained by derivating equations 6 with respect to s , reporting then equations 4. Eliminating finally ψ by using once more equations 6, we get:

$$\begin{cases} \underline{Z}' &= A \underline{Z} + B \delta \\ y &= C \underline{Z} \end{cases} \quad (7)$$

$$\text{with : } A = \begin{bmatrix} -\frac{\xi_2}{\xi_1} & -\frac{\xi_3}{\xi_1} \\ \frac{\xi_2}{\xi_1 \xi_3} & \frac{\xi_2}{\xi_1} \end{bmatrix} \quad B = \begin{bmatrix} 0 \\ \frac{1}{L \xi_3} \end{bmatrix}$$

In the sequel, 2 output functions are investigated : $y = a$ and $y = b$. The associated output vectors, are respectively $C = [1 \ 0]$ and $C = [0 \ 1]$.

3 Control

Line following can be conducted from the image frame by regulating either a or b : in view of 6 and 4, the convergence of x and ψ , to respectively x^* and 0, follows from those of a to $a^* = \frac{x^*}{\xi_1}$, or from those of b to $b^* = -\frac{\xi_2}{\xi_1 \xi_3} x^*$. Since the state space model of the application is linear, the regulation of a or b can be achieved by assigning the poles of the output error dynamics. This approach, investigated in Section 3.1, demonstrates however weak capacities in presence of modelling errors. In order to improve control robustness, we then turn towards \mathcal{H}_∞ control in Section 3.2.

3.1 Pole assignment control

Let y^* denote the desired constant output value. The following transfer function 8 can be imposed by designing the control law as presented in relation 9.

$$\frac{Y(p)}{Y^*(p)} = \frac{Num(p)}{(p^2 + 2\xi\omega_0 p + \omega_0^2)(p + \xi\omega_0)} \quad (8)$$

$$\delta = [-k_1 \quad -k_2] \underline{Z} - k_i \int (y^* - y) ds \quad (9)$$

where $Num(p)$ represents a polynomial of degree 0 when $y = a$, and of degree 1 when $y = b$. The relation between the gains (k_1, k_2, k_i) and the desired dynamics (ξ, ω_0) can be derived using the same approach than those presented in [11].

When no modelling error is assumed, the regulation of a or b leads to identical results. On the contrary, when the camera inclination angle α is perturbed, model parameter ξ_2 is then unperfectly known. Convergence of a or b to respectively a^* or b^* can still be achieved when integrators are used, as in 9. However, convergence of x to x^* is obtained only when the output variable is a , see relations 6.

Results

The vision system computes the (a, b) parameters of the projected line in the image plane at video rate, and a data flow latency of three sample periods has been identified.

We only present the best results (Figures 3 and 4) obtained when using the pole assignment technique with integrator and the parameter a as the output of the system. The dynamic parameters ξ and ω_0 have been set respectively to 0.9 and 2 rd/s. The nominal velocity V has been chosen equal to 20 km.h⁻¹.

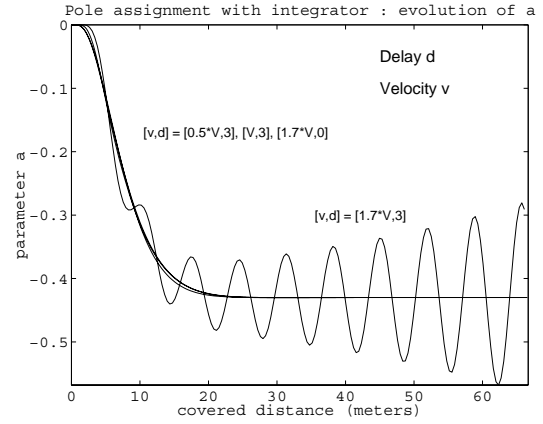


Figure 3: Influence of the data flow latency

Figure 3 illustrates the influence of the data flow latency. Since the imposed output error dynamic 8 is a spatial one, the vehicle trajectory, when converging to the reference line, should be identical whatever the vehicle velocity is. This feature is verified when the velocity is V or $\frac{V}{2}$. The slight error only follows from the unmodelled delay. On the contrary, for higher velocities, oscillations appear, and divergence finally occurs when the velocity is $1.7V$. A fourth simulation, with velocity $1.7V$ and zero delay, has been run. The vehicle trajectory is again superposed with those obtained at lower velocities. This demonstrates that the data flow latency, not addressed during the control design, is the only responsible for the above-observed divergence.

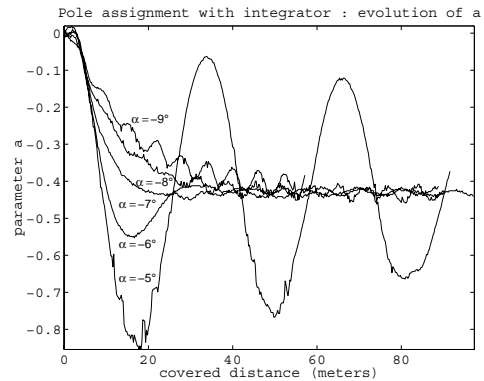


Figure 4: Evolution of a

In Figure 4, we present the output behaviour when we introduce perturbations on the camera inclination angle. Oscillations and instability occur even for a weak variation of α ($\pm 2^\circ$). Due to these problems, we have decided to investigate a robust control approach.

3.2 Robust control

We chose the approach developed in \mathcal{H}_∞ space at the beginning of the eighties [18, 10, 5, 6, 4], concerning controller design with plant uncertainties modelled as unstructured additive perturbations in the frequency domain.

3.2.1 Generality on \mathcal{H}_∞ control

The servoing scheme is presented in the Figure 5 .

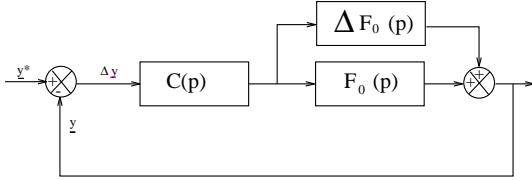


Figure 5: Servoing scheme in \mathcal{H}_∞ space

We consider an additive perturbation in the frequency domain :

$$F(p) = F_0(p) + \Delta F_0(p) \quad (10)$$

where $F_0(p)$ represents the nominal transfer function.

The aim is to determine a single robust controller $c(p)$ which ensures the stability of the closed loop system. Then, we can write $1 + F(p).c(p)$ as:

$$\begin{aligned} & [1 + F_0(p).c(p)] \cdot \left[1 + \frac{c(p)}{1 + F_0(p).c(p)} \cdot \Delta F_0(p) \right] \\ & = [1 + F_0(p).c(p)] \cdot [1 + q(p) \cdot \Delta F_0(p)] \end{aligned} \quad (11)$$

$$\text{with } q(p) = \frac{c(p)}{1 + F_0(p).c(p)}.$$

To ensure the stability of the closed loop system, we must verify:

$$|1 + F(j\omega).c(j\omega)| \neq 0 \quad \forall \omega \quad (12)$$

We define a transfer function $r(j\omega)$ which bounds the variations of $F_0(j\omega)$ as:

$$\begin{cases} |\Delta F_0(j\omega)| \leq |r(j\omega)| \\ \frac{|r(j\omega)|}{|F_0(j\omega)|} \leq 1 \end{cases} \quad \forall \omega \quad (13)$$

In this case, if $c(p)$ stabilizes the nominal plant $F_0(p)$ we can express the robust stability condition as [10] :

$$\|q(p)r(p)\|_\infty < 1 \quad (14)$$

In these conditions, the robust controller can be expressed by :

$$c(p) = \frac{q(p)}{1 - F_0(p)q(p)} \quad (15)$$

Plant with two poles at the origin

In this part we summarize the different steps to follow to synthesize a robust controller when the plant comprises two poles at the origin [10, 4, 1].

We construct the proper stable function:

$$\widetilde{F}_0(p) = p^2 \cdot B(p) \cdot F_0(p) \quad (16)$$

where $B(p) = \prod \left(\frac{p_i - p}{p_i + p} \right)$ represents the Blaschke product of unstable poles p_i ($Re(p_i) > 0$) of $F_0(p)$.

For convenience, we define $\tilde{q}(p)$ as:

$$\tilde{q}(p) = \frac{q(p)}{p^2 \cdot B(p)} \quad (17)$$

and then:

$$F_0(p) \cdot q(p) = \widetilde{F}_0(p) \cdot \tilde{q}(p) \quad (18)$$

We have to choose a minimal phase function $r'_m(p)$ as:

$$r(p) = \frac{r'_m(p)}{p^2} \quad (19)$$

where $r(p)$ bounds the variations of the nominal plant $F_0(p)$.

The robust condition of stability can be rewritten as:

$$\|u(p)\|_\infty < 1 \quad \text{with } u(p) = \tilde{q}(p) \cdot r'_m(p) \quad (20)$$

Since the function $1 - F_0(p).q(p)$ has the zeros at the unstable poles α_i of $F_0(p)$, and using relation 18, we can express the first interpolation conditions with:

$$\tilde{q}(\alpha_i) = \frac{1}{\widetilde{F}_0(\alpha_i)} \quad \forall i = 1, \dots, l \quad (21)$$

We can write the second condition of interpolation at the origin :

$$\tilde{q}(0) = \frac{1}{\widetilde{F}_0(0)} \quad 2 \text{ poles at the origin} \quad (22)$$

Since $\tilde{q}(p)$ and $r'_m(p)$ are \mathcal{H}_∞ functions, the function $u(p) = r'_m(p) \cdot \tilde{q}(p)$ must be an SBR function (Strictly Bounded Real), and the conditions of interpolation can be written as:

$$\begin{cases} u(\alpha_i) = \frac{r'_m(\alpha_i)}{\widetilde{F}_0(\alpha_i)} \quad \forall i = 1, \dots, l \\ u(0) = \frac{r'_m(0)}{\widetilde{F}_0(0)} \quad 2 \text{ poles at the origin} \end{cases} \quad (23)$$

So the solution to the problem of robust stabilization of an unstable system [10] lies in finding an SBR function $u(p)$ which interpolates to the points $u(\alpha_i)$. This problem is called the Nevanlinna-Pick interpolation problem. Dorato *et al* in [5] have proposed an iterative solution to this problem based on the interpolation theory of Youla-Saito [17]. When the relative degree of the function $r'_m(p)$ is greater than 0, we must append one or more supplementary interpolation conditions near infinity.

3.2.2 Robust lateral controllers

We have used \mathcal{H}_∞ approach to design lateral controllers with both parameters a and b .

Controller design using parameter b

When parameter b is considered as the output of the system, from 4 and 6 we have:

$$\begin{cases} F_1(p) = \frac{b}{\delta} = \frac{\xi_2 + p\xi_1}{\xi_1 p^2 L \xi_3} \\ \frac{\Delta F_1(p)}{F_1(p)} = \frac{|\frac{\Delta \alpha}{\alpha}| + |\frac{\Delta h}{h}|}{1 + \frac{\xi_1}{\xi_2} p} \end{cases} \quad (24)$$

Using the following expression of $r(p)$:

$$r(p) = \sup_{\omega} \left| \frac{\Delta F_1(j\omega)}{F_1(j\omega)} \right| F_1(p) \quad (25)$$

we can consider $r'_m(p)$ as:

$$r'_m(p) = K_1 \cdot p^2 \cdot F_1(p) \quad (26)$$

We set the range of variations of $\frac{\Delta \alpha}{\alpha}$ and $\frac{\Delta h}{h}$ respectively to 0.57 and 0.25. Therefore, we deduce from 24 and 26 that $K_1 = 0.82$.

Since $F_1(p)$ has no unstable pole, the function $B(p) = 1$, and we have to choose $u(p)$ as an SBR function with a relative degree of 1 (because of the expression of $r'_m(p)$).

We choose the following expression of $u(p)$:

$$u(p) = \frac{K_1}{1 + \tau \cdot p} \quad (27)$$

to satisfy the conditions of interpolation:

$$\begin{cases} u(0) = \frac{r'_m(0)}{F_1(0)} = K_1 \quad \text{at the origin} \\ u(\infty) = 0 \end{cases} \quad (28)$$

Developing, we obtain the robust controller $c(p)$:

$$c(p) = \frac{\xi_1 p L \xi_3}{\tau \cdot (\xi_2 + p \xi_1)} \quad (29)$$

Controller design using parameter a

When parameter a is the output of the system, we have:

$$\begin{cases} F_2(p) = \frac{a}{\delta} = -\frac{1}{\xi_1 L p^2} \\ \frac{\Delta F_2(p)}{F_2(p)} = \left| \frac{\Delta h}{h} \right| \end{cases} \quad (30)$$

As previously, we use the same expression for $r(p)$ and looking at the expression of $F_2(p)$, we can consider $r'_m(p)$ as:

$$r'_m(p) = K_2 \cdot p^2 \cdot F_2(p) \quad \text{with } K_2 = 0.25 \quad (31)$$

Since $F_2(p)$ has no unstable pole, we have to choose $u(p)$ as an SBR function with a relative degree of 2.

We choose the following expression of $u(p)$:

$$u(p) = \frac{K_2}{(1 + \tau p)^2} \quad (32)$$

and writing the conditions of interpolation at the origin and at infinity, we obtain the expression of the robust controller $c(p)$:

$$c(p) = -\frac{\xi_1 L p}{\tau \cdot (2 + \tau p)} \quad (33)$$

3.2.3 Results

To evaluate robust control, we have used the same tests than in section 3.1. In addition, we have considered perturbations on camera height.

Influence of the data flow latency

Figure 6 illustrates that the \mathcal{H}_∞ controller is less sensitive to unmodelled delay than the classical poles assignment law: when the vehicle velocity is 1.7V, its

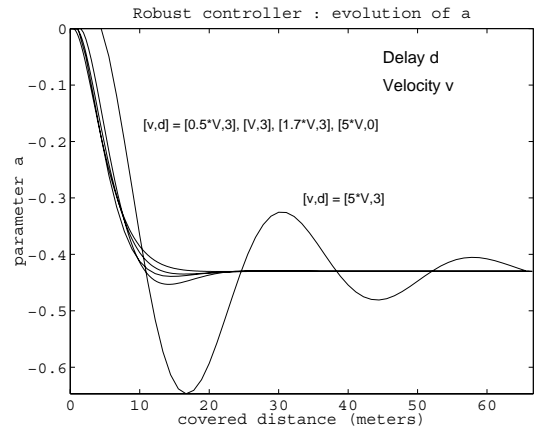


Figure 6: Influence of the data flow latency

trajectory is this time still close to the nominal one. Simulations with higher velocities, up to $5 V$, have also been successively run. Severe oscillations occur, but the vehicle still converges to the reference line.

Perturbations on angle α

We have successively chosen as output variable b , Figure 7 ($b^* = 100 \text{ pixels}$, $\tau = 0.67$), and a , Figure 8 ($a^* = 0.43$, $\tau = 0.5$).

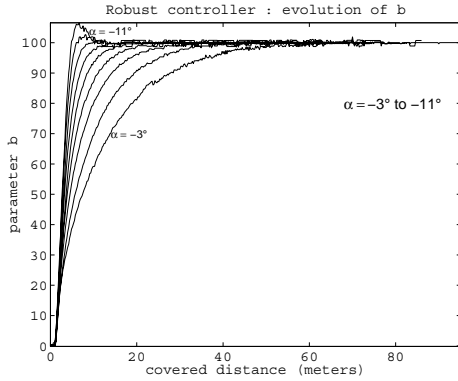


Figure 7: Evolution of b

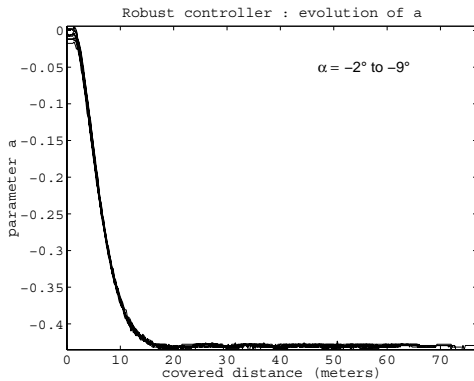


Figure 8: Evolution of a

In both cases, the robustness is much improved with regard to pole assignment: no oscillation is noticed even with $\Delta\alpha \in [-2^\circ; +5^\circ]$. Moreover, contrarily to the use of b , the vehicle trajectory is not altered when a is the output variable. We have also verified that, as expected, there is no steady state error on the lateral position x , when using the a parameter.

Coupling perturbations

In the final test, we have combined perturbations into camera height and camera inclination angle. Using the parameter a as the output of the system, we have compared the pole assignment and robust control

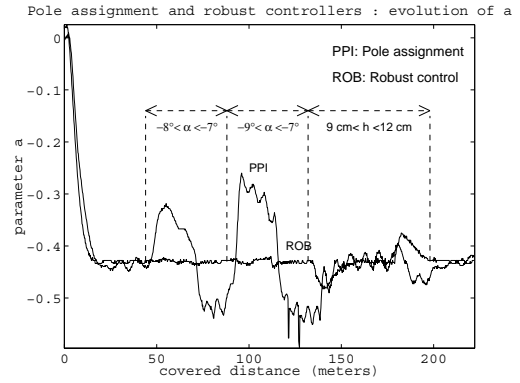


Figure 9: Evolution of a

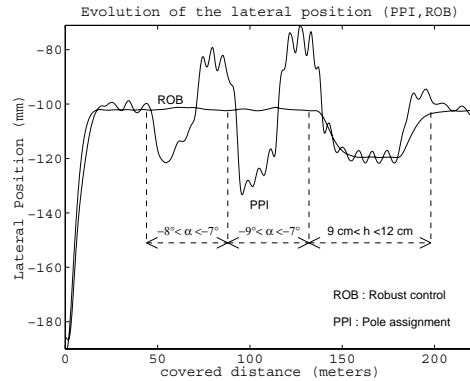


Figure 10: Evolution of x

approaches. Figures 9 and 10 present respectively the evolution of a and x .

When we introduce perturbations on camera height, a still converges to a^* , but a steady state error appears on x due to the presence of h in ξ_1 , see 6.

4 Conclusion

In this paper we have shown how to synthesize lateral controller in sensor space for AGV applications. In a first part, we develop the modelling of the vehicle taking into account a normalization with the longitudinal velocity. In these conditions, we establish a state model of the system and deduce a first control approach based on pole assignment. We show that the choice of a instead of b parameter to design controllers is much adapted in presence of perturbations. Oscillations and instability occur at high velocities due to the presence of a pipeline delay in the closed loop control. In addition, the same phenomenon can be observed when we have weak variations of plant uncertainties.

So we decide to investigate a robust control approach. The presented robust controllers are efficient with regard to delay and to plant uncertainties, except for the camera height.

In the future, we intend to solve this latter problem, and we want to adapt this control scheme in order to take also into account perturbations into the camera roll angle. Finally, an extension of these work can be done in designing dynamic robust lateral controllers taking into account a dynamic model of the vehicle.

References

- [1] R.H. Byrne and A. Chaouki. Robust lateral control of highway vehicles. In *Proceedings of Intelligent Vehicle Symposium*, pages 375–380, Paris, France, October 1994.
- [2] R. Chapuis, A. Potelle, J.L. Brame, and F. Chausse. Real-time vehicle trajectory supervision on the highway. *The International Journal of Robotics Research*, 14(6):531–542, December 1995.
- [3] E.D. Dickmanns and A. Zapp. Autonomous high speed road vehicle guidance by computer. In *Proceedings of 10th IFAC World Congress*, July 1987.
- [4] P. Dorato, L. Fortuna, and G. Muscato. *Robust Control for Unstructured Perturbations-An Introduction*, volume 168. Springer-Verlag, Lectures Notes in Control and Information Sciences, 1992.
- [5] P. Dorato and Yunzhi Li. A modification of the classical Nevanlinna-Pick interpolation algorithm with applications to robust stabilization. *IEEE Transactions on Automatic Control*, 31(7):645–648, July 1986.
- [6] J. Doyle, K. Glover, P. Khargonekar, and B. Francis. State space solutions to standard H_2 and H_∞ control problems. *IEEE Transactions on Automatic Control*, 34(8), 1989.
- [7] F. Jurie, P. Rives, J. Gallice, and J.L.Brame. High-speed vehicle guidance based on vision. *Control Engineering Practice*, 2(2):287–297, December 1994.
- [8] N. Kehtarnavaz, N.C. Grisworld, and J.S. Lee. Visual control for an autonomous vehicle (bart)-the vehicle following problem. *IEEE Transactions on Vehicular Technology*, 40(3):654–662, August 1991.
- [9] D. Khadraoui, P. Martinet, and J. Gallice. Linear control of high speed vehicle in image space. In *Proceedings of Second International Conference on Industrial Automation*, volume 2, pages 517–522, Nancy , France, June 1995.
- [10] H. Kimura. Robust stabilization for a class of transfer fonction. *IEEE Transactions on Automatic Control*, 29:788–793, September 1984.
- [11] P. Martinet, D. Khadraoui, C. Thibaud, and J. Gallice. Controller synthesis applied to automatic guided vehicle. In *Proceedings of Fifth Symposium on Robot Control*, volume 3, pages 735–742, Nantes , France, September 1997.
- [12] P. Martinet, C. Thibaud, D. Khadraoui, and J. Gallice. First results using robust controller synthesis in automatic guided vehicles applications. In *Proceedings of Third IFAC Symposium on Intelligent Autonomous Vehicles*, volume 1, pages 204–209, Madrid , Spain, March 1998.
- [13] R. Pissard-Gibollet and P. Rives. Asservissement visuel appliqué à un robot mobile: état de l’art et modélisation cinématique. Technical Report 1577, INRIA, December 1991.
- [14] C. Samson, M. Le Borgne, and B. Espiau. *Robot Control: The task function approach*. ISBN 0-19-8538057. Oxford University Press, 1991.
- [15] R. Wallace, K Matsuzak, Y. Goto, J. Crisman, J. Webb, and T. Kanade. Progress in robot road following. In *Proceedings of the IEEE International Conference on Robotics and Automation*, April 1986.
- [16] A.M. Waxman, J. LeMoigne, L.S Davis, B. Srinivasan, T.R. Kushner, E. Liang, and T. Siddalingaiah. A visual navigation system for autonomous land vehicles. *IEEE Transactions on Robotics and Automation*, 3(2):124–141, 1987.
- [17] D.C. Youla and M. Saito. Interpolation with positive-real functions. *J. Franklin Inst.*, 284(2):77–108, 1967.
- [18] G. Zames and B.R. Francis. Feedback, minimax sensitivity, and optimal robustness. *IEEE Transactions on Automatic Control*, AC-28(5):585–601, May 1983.